



ELSEVIER

1 October 1995

OPTICS  
COMMUNICATIONS

Optics Communications 120 (1995) 78–74

## A second order nonlinear lens parametrization with a Ti:sapphire laser

G. Toci<sup>1,a</sup>, M. Vannini<sup>b</sup>, R. Salimbeni<sup>b</sup>, R. Pini<sup>b</sup><sup>a</sup> Dipartimento di Fisica, L. go Enrico Fermi 2, 50125 Firenze, Italy<sup>b</sup> Istituto di Elettronica Quantistica del CNR, Via Panciatichi 56/30, 50127 Firenze, Italy

Received 11 April 1995

### Abstract

We report a second order lens effect detection in the 100 fs time region achieved in a LBO crystal with a Ti:sapphire laser. We implemented the already reported steady state theory which takes into account both the phase and amplitude modulation of the fundamental field affecting its subsequent propagation. We compare this lens effect with the classical Kerr effect with the purpose of realizing a passive modulation device evidencing the advantages of a stronger effect and the possibility of adjusting the magnitude and sign.

### 1. Introduction

Recently it was demonstrated that large, intensity dependent amplitude and phase modulation on optical beams can be induced by second order optical nonlinearities [1–3]. In particular, during the propagation through a frequency doubling crystal, an optical wave can experience phase or amplitude modulations under the influence of an injected second harmonic signal.

Research on this effect has two main purposes: (1) obtaining an efficient all-optical switching action in guided propagation [4]; (2) achieving an efficient intensity dependent self-modulation of the incident beam, that can be used to get a passive mode-locking operation of a broadband cw laser source.

Mode locking action with a double pass second order process was realized by Stankov [5] with the nonlinear mirror, whose operation is based on the amplitude mod-

ulation which the fundamental beam undergoes during the two passes in phase-matching conditions through the doubling crystal. This is due to the fundamental depletion and subsequent repumping by the beam at  $2\omega$ , achieving a saturable absorber effect.

Besides the amplitude modulation effects, an intensity-dependent phase shift on the fundamental beam can be obtained in phase matching conditions, by means of a suitable control of the phase difference of the  $\omega$  and the  $2\omega$  fields injected into the doubling crystal [3]. This is the degenerate case of the more general nondegenerate three-wave parametric interaction, which exhibits a  $\chi^{(2)}$  induced cross-phase modulation. In particular, the resulting intensity-dependent phase shift on a fundamental beam with transverse intensity modulation results in an overall self-focusing action (parametric lens effect), similar to the classical Kerr-lens effect, but with an adjustable magnitude and sign.

The aim of this work is to define a frame for a complete theoretical description and to provide an experimental characterization of the parametric lens effect on

<sup>1</sup> Research performed at the Istituto di Elettronica Quantistica del CNR

gaussian beams arising in a double pass second harmonic generation process, in phase-matching conditions, with the perspective of employing the effect as an intracavity modulation device suitable for passive mode-locking. Depending on the relative phase difference of the injected fields the second order process produces a self focusing and a self-aperturing action on the fundamental beam, this last properly introduced here for the first time, both determining the spatial properties of the fundamental beam at the output.

The parametric lens and aperture effects were experimentally studied as a result of a double pass second harmonic generation process in a LBO crystal, excited with a passively mode-locked Ti:sapphire laser. By properly balancing the pulse duration and the crystal length the experiment is set in a temporal region where the process arises at the border of a quasi-stationary interaction. In fact as it has been pointed out in [7,8] the ultimate limits of the temporal selectivity of a passive modulator based on a second order process are determined by the effects of the group velocity mismatch (GVM) between the fundamental and the harmonic pulse into the crystal.

With a proper choice of the doubling crystal parameters it is possible to achieve significant intensity dependent modulation effects, even higher than those reached by the usual Kerr media.

## 2. Theory

The main outlines of the theory in stationary conditions were already exposed in [3]. It is worth to recall here the principal results.

The magnitude of the phase and amplitude modulation experienced by the interacting field  $\rho_1$  and  $\rho_2$  can be found from the well known Bloembergen equations [8] describing the degenerate three-wave parametric interaction:

$$\frac{d\rho_1}{dz} = iK\rho_1^* \rho_2, \quad (1a)$$

$$\frac{d\rho_2}{dz} = iK\rho_1^2, \quad (1b)$$

where  $K = 4\pi k_1 \chi_{\text{eff}}^{(2)} / n_1^2$  is the nonlinear coupling constant,  $\chi_{\text{eff}}^{(2)}$  is the appropriate second order susceptibility tensor element,  $k_1$  is the fundamental wave number,  $n_1$

is the refraction index at  $\omega$ . We will assume that at the input of a nonlinear medium of length  $L$  it is  $\rho_1(z=0) = \rho_{10} e^{i\phi_{10}}$ ,  $\rho_2(z=0) = \rho_{20} e^{i\phi_{20}}$ , with  $\rho_{10}$ ,  $\rho_{20}$  real values.

In the limit of low conversion efficiency the coupled equations (1a), (1b) can be solved by expanding the fields in power of the single pass field conversion efficiency  $\eta = KL\rho_{10}$ , without second harmonic signal injected. The complex field amplitudes at the output of a crystal of length  $L$  are given by

$$\begin{aligned} \rho_1(L) &= \rho_{10} e^{i\phi_{10}} \\ &\times \left[ 1 + \frac{\rho_{20}}{\rho_{10}} \eta (\sin \Theta - i \cos \Theta) - \left( 1 - \frac{\rho_{20}^2}{\rho_{10}^2} \right) \frac{\eta^2}{2} \right], \end{aligned} \quad (2a)$$

$$\rho_2(L) = \rho_{20} e^{i\phi_{20}} \left[ 1 + \frac{\rho_{10}}{\rho_{20}} \eta (\sin \Theta - i \cos \Theta) - \eta^2 \right], \quad (2b)$$

up to the second order in  $\eta$ , where  $\Theta = \phi_{20} - 2\phi_{10}$  is the relative phase difference at the second pass input.

Eqs. (2a), (2b) show that during the propagation into the crystal both fields experience a phase or an amplitude modulation whose magnitude and sign depends on their instantaneous amplitude and on their relative phase difference  $\Theta$  at the crystal input.

The physical origin of the nonlinear phase shift is that the fundamental field at the output of the second pass originates from the superimposition of the injected fundamental field and from the contribution of the downconverted second harmonic, whose relative phase depends from the phase of the harmonic field. The amplitude and/or phase modulation experienced by the fundamental field is proportional to the injected second harmonic field.

In our experimental set up, the second harmonic field is generated during a first pass into the crystal with a conversion efficiency  $\eta$ ; then both fields are reinjected into the crystal, taking into account of the reflection losses  $r_1$ ,  $r_2$ , respectively. The amplitude of the injected second harmonic field is then given by

$$\rho_{20} = (r_2/r_1^2) KL\rho_{10}^2 = (r_2/r_1) \eta \rho_{10}, \quad (3)$$

where we neglected the pump depletion effect during the first pass.

For interacting beams of finite aperture, the radial dependence of the phase and amplitude modulation

result respectively in a lensing and in a aperture effect on the fundamental beam.

Considering a fundamental gaussian beam with beam waist radius  $w_{10}$ , Rayleigh range  $z_R$ , peak amplitude  $\rho_{1pk}$ , the  $2\omega$  beam generated during the first pass remains gaussian with the same  $z_R$  value and  $w_{20} = w_{10}/\sqrt{2}$ . Assuming that during the second pass the two beams are matched, with the nonlinear crystal much thinner than  $z_R$ , at the output of the crystal the fundamental beam amplitude and its relative phase change due to the nonlinear interaction are given by

$$|\rho_1(r, L)| = |\rho_{1pk}| \exp(-r^2/w_1^2) \times [1 - (r_2/r_1^2) \eta_{pk}^2 \exp(-r^2/w_2^2) (r_1^2/r_2 + \sin\Theta)], \quad (4)$$

$$\Delta\phi_{1NL} = -(r_2/r_1^2) \eta_{pk}^2 \exp(-r^2/w_2^2) \cos\Theta, \quad (5)$$

up to the second order in  $\eta_{pk}$ , single pass field conversion efficiency at the peak of the gaussian distribution.

Due to the radial dependence of the injected second harmonic field, the phase and the amplitude profile show a radial dependence determining a lensing effect of the fundamental beam, already described in the previous work [3], and a gaussian aperture effect, previously unnoticed, that should be taken into account to obtain an accurate description of the process.

The effect produced on the beam propagation by the superimposed phase and amplitude modulation can be described by means of the ‘‘Gaussian decomposition’’ method applied by Sheik-Bahae et al. [9] in the frame of the  $z$ -scan technique, which accounts for the gaussian profile of the perturbation.

The conversion efficiency depends from the crystal position as

$$\eta_{pk}^2(x) = \eta_0^2 / (1 + x^2), \quad (6)$$

where  $x = Z/z_R$  is the crystal distance from the beam waist (in units of Rayleigh range),  $\eta_0$  is the single pass conversion efficiency at the peak of the gaussian distribution and at the beam waist.

With this method, keeping up to the first order in  $\eta_0^2$ , according to [9] the central intensity of the fundamental beam in the far field at the output of the crystal is found to be

$$I_0(\Theta, x) = 1 + \eta_0^2 (r_2/r_1^2) \frac{[4x \cos\Theta - 2(x^2 + 3) \sin\Theta]}{(x^2 + 1)(x^2 + 9)} \quad (7)$$

resulting from the cumulative effect of the nonlinear phase and amplitude modulation on the beam propagation and from the overall pump beam power depletion. This latter can be canceled if we consider the transmission through a small pinhole in the beam far field, as calculated with respect to the total fundamental power at the output of the crystal. The total output power is given by

$$P_1(\Theta, x) = P_{10} [1 - (r_2/r_1^2) \eta_{pk}^2(x) \sin\Theta] \quad (8)$$

and thus the transmission

$$T(\Theta, x) = 1 + \eta_0^2 (r_2/r_1^2) \frac{[4x \cos\Theta - 2(3 - x^2) \sin\Theta]}{(x^2 + 1)(x^2 + 9)} \quad (9)$$

at the first order in  $\eta_0^2$ , normalized with respect to its  $\Theta$ -averaged value. It is worth to note that the transmission is dephased in  $\Theta$  with respect to the total power (Eq. (8)), because the amplitude modulation (i.e., the soft aperture action) and the phase modulation (i.e. the lens power) are in phase quadrature with respect to  $\Theta$ , and their effect on the beam transmission has a different weight depending on the crystal position  $x$ . The resulting dephasing angle depends on the crystal position according to the following equation:

$$\sin\Theta_T(x) = 4x [16x^2 + (3 - x^2)^2]^{-1/2}, \quad (10)$$

that is independent from the conversion efficiency  $\eta_0^2$ .

The theory exposed before is valid only in stationary conditions of interaction between the fundamental and the harmonic pulse, which is satisfied if the fundamental pulse duration is of the same order of magnitude or greater than the propagation delay between the fundamental and the second harmonic pulse along the crystal thickness, due to their GVM [6,7]. In the frequency domain, this condition is fulfilled when the crystal phase-matching bandwidth is greater than the laser pulse spectral width.

When dealing with subnanosecond pulsed laser sources, it becomes very difficult to measure the time-resolved transmission as described by the Eq. (9); when considering instead the time-averaged transmission, the Eq. (9) has to be modified by replacing the instantaneous conversion efficiency (at the beam waist and at the spatial and temporal peak of the intensity distribution)  $\eta_0^2$  with its time-averaged value, that for a gaussian pulse shape is given by  $\bar{\eta}_0^2 = \eta_0^2/\sqrt{2}$ ; fur-

thermore, for a  $TEM_{00}$  beam the time-averaged conversion efficiency  $\bar{\eta}_0^2$  at the spatial peak of the intensity distribution is related to the space-time averaged conversion efficiency (i.e., the total average power conversion efficiency)  $\langle \bar{\eta}_0^2 \rangle$  through the following relation:  $\langle \bar{\eta}_0^2 \rangle = \bar{\eta}_0^2/2$ .

### 3. Experimental set up and measurements

The parametric lens effect was detected as resulting from a double pass harmonic generation process in a LBO crystal, excited by a Ti:sapphire laser beam.

The laser source is a commercial (Lexel 480 Avante') Ar<sup>+</sup> pumped Ti:sapphire laser, oscillating in Kerr lens self mode locking regime, (average power 550 mW at 790 nm, pulse repetition frequency 100 MHz, pulse duration 180 fs fwhm assuming a sech<sup>2</sup> pulse shape, band width 4.0 nm fwhm, almost  $TEM_{00}$  mode).

The nonlinear crystal is a 1 mm thick LBO, cut for type I phase matched second harmonic generation with minimum lateral walkoff angle at 790 nm. At this wavelength the propagation delay due to the GVM (as can be calculated from the refraction index data, [10]) is about 120 fs/mm along the phase matching curve, and the phase matching band width is about 7.2 nm/mm fwhm [11], fulfilling the conditions for a quasi-stationary interaction.

The experimental set-up (Fig. 1) has been designed to minimize the use of dispersive optical elements along the beam path, and to allow a proper compensation of the propagation delay between the first and the second pass.

The Ti:sapphire laser beam is focused into the LBO crystal by the mirror M1 ( $f=5$  cm), with a  $z_R=1.45$  mm, as determined with a  $z$ -scan measurement of the

single pass conversion efficiency, corrected for the crystal thickness; measuring the beam diameter on the focusing mirror plane with a CCD camera allows to calculate the value of the beam quality factor  $M^2=1.1$ , indicating that the beam is quite gaussian [12]. The Rayleigh range of the beam into the crystal is given by  $z_R'=z_R \times n_1=2.45$  mm, thus fulfilling the condition  $z_R'>L$ . The beam is then recollimated by the mirror M2 and sent to the Michaelson interferometer formed by the harmonic separator HS, and the mirrors MH and MF. MH is mounted on a double coaxial movement (motorized and piezo translator) allowing respectively to compensate for the propagation delay between the  $\omega$  and the  $2\omega$  pulse due to the GVM along the overall optical path, and to modulate the phase difference  $\theta$ . The overall reflectivities of the interferometer arms are  $r_1=0.93$  and  $r_2=0.89$ . The beam is then focused back for the second pass into the crystal to undergo the cross-phase modulation process. Without second harmonic signal injected, conversion efficiency for the average power  $\langle \bar{\eta}_0^2 \rangle$  during the second pass is about 5% with the crystal on the beam waist. The two pass are slightly misaligned to prevent the output beam to enter in the laser cavity.

After recollimation on M1, the beam is picked up by the beam splitter BS and sent to the photodiode PD1, measuring its central intensity  $I_0$  as selected by the iris I, whereas the remaining part of the beam reaches the photodiode PD2 measuring the fundamental total power  $P_0$ . The second harmonic is rejected by means of dichroic filters. The photodiode signals are recorded by a digitizing oscilloscope.

With this experimental set-up it is possible to determine the effect produced on the fundamental beam propagation by the injected second harmonic signal, for different values of the input phase difference and of the crystal position along the beam path.

Fig. 2a shows a typical scan trace of the beam total power  $P_0$  (providing a reference signal for the input phase difference, as given by Eq. (7)) and of its central intensity in dependence of the input phase difference  $\theta$  ( $\theta$ -scan). The central intensity variations are caused both by the variations of the total power and the spot size. Their relative dephasing angle with respect to (Fig. 2b) evidences the presence of a spot size variation in that in turns is dephased with respect to  $P_0$ .

From the photodiode signals shown in Fig. 2a it is possible to calculate the relative transmission variations

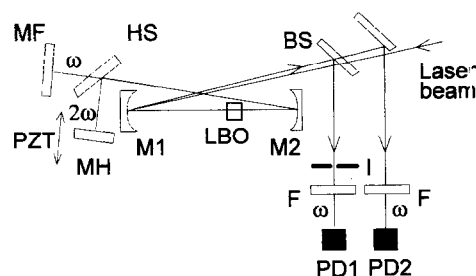


Fig. 1. The experimental set-up.

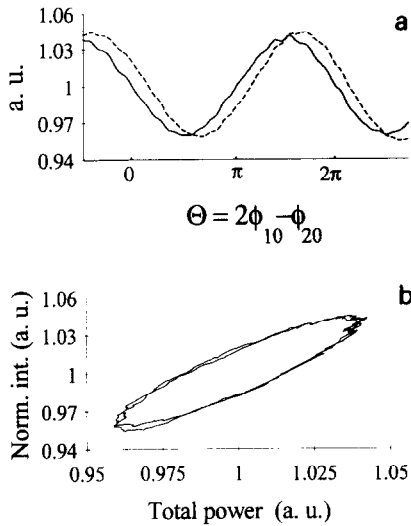


Fig. 2.  $\Theta$ -scan trace of the average total power  $P_0(\Theta)$  (solid line) and average central intensity  $I_0(\Theta)$  (dashed line) at  $Z=1.5$  mm. (b) Lissajous diagram of the central intensity  $I_0(\Theta)$  versus the total power  $P_0(\Theta)$ .

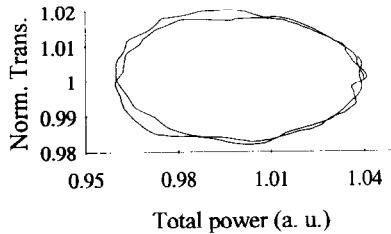


Fig. 3. Average transmission  $T(\Theta)$  of the fundamental beam through the iris versus the total power  $P_0(\Theta)$  as calculated from the traces of Fig. 2a.

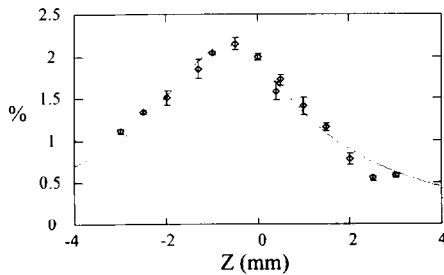


Fig. 4. Relative modulation amplitude of the transmission  $T(\Theta)$ , for various positions of the crystal along the beam path. The solid line is the best fit of Eq. (9).

through the iris due to the nonlinear lens and aperture effect when the input phase difference is changed.

Fig. 3 shows a typical  $\Theta$ -scan trace of the transmission  $T(\Theta)$  versus the beam total power as can be calculated from the traces shown in Fig. 2a, b, allowing to measure the modulation amplitude of the transmission and its phase difference in  $\Theta$  with respect to the total power.

#### 4. Discussion

To give a complete description, the parametric effect has to be characterized in terms of spot size modulation amplitude and dependence from the field input phase difference  $\Theta$ . The measurements have to be compared with the results of the theoretical model.

Fig. 4 shows, for different positions of the crystal along the beam, the relative modulation amplitude of the transmission through the iris with respect to  $\Theta$  as it can be calculated from experimental data. The solid line is the best fit of the amplitude that can be calculated from Eq. (9), obtained with fitting values of  $z_R$  and  $\eta_0^2$  very close to the actually observed values. The error bars represent the standard deviations for several cycles in  $\Theta$ .

The dependence of the transmission from the phase difference  $\Theta$  can be tested considering the behavior of the phase difference  $\Theta_T(x)$  between the transmission and the total power (cf. Eq. (10)). Fig. 5 shows the observed values of  $\sin \Theta_T(x)$  for various crystal positions, fitted with Eq. (10). The only fitting parameter is the value of  $z_R$  which results in good agreement with the value determined with the  $z$ -scan measurement of the single pass conversion efficiency. In both cases the agreement with the theory is quite good.

The separation of the contributions on the transmission of the soft aperture effect and of the lens effect can

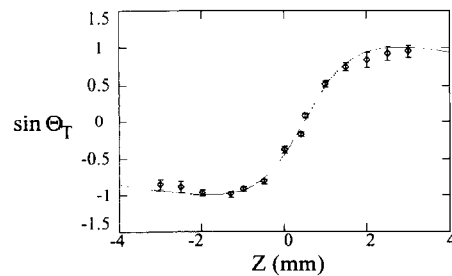


Fig. 5. Relative dephasing angle  $\Theta_T(Z)$  between the transmission  $T(\Theta)$  and the total power  $P_0(\Theta)$ , for various positions of the crystal along the beam path. The solid line is the best fit of Eq. (10).

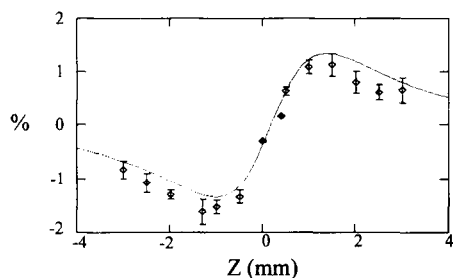


Fig. 6. Relative central intensity variation due to the aperture effect ( $\Theta=0$ ) for various positions of the crystal along the beam path.

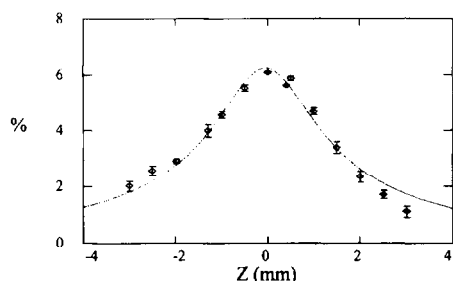


Fig. 7. Relative central intensity variation due to the lens effect ( $\Theta=\pi/2$ ) for various positions of the crystal along the beam path.

be achieved owing to their different dependence with respect to  $\Theta$ . Fig. 6 and Fig. 7 show the  $z$ -scan of the relative central intensity  $I_0$  (i.e. the transmission as measured with respect to the input beam) with  $\Theta=0$  (only aperture effect) and with  $\Theta=\pi/2$  (only lens effect) respectively. The solid lines are the fits obtained from Eq. (7).

Within the perspective of exploiting this effect to realize an ultrafast passive optical modulator suitable for the passive mode locking of a laser source, the parametric lens effect has to be compared with the self focusing effect arising in a Kerr medium. The nonlinear phase shift experienced by the fundamental beam at the output of the second pass (cf. Eqs. (3), (5)) is given by

$$\begin{aligned} \Delta\phi_{\text{INL}} &= -(r_2/r_1^2) \eta_{\text{pk}}^2 = (r_2/r_1^2) (4\pi k_1 \chi_{\text{eff}}^{(2)}/n_1^2)^2 L^2 \rho_{\text{1pk}}^2 \\ &= -0.18, \end{aligned} \quad (11)$$

where the numerical value has been evaluated from the observed transmission modulation at  $x=0.86$ , corresponding to the maximum effect on the beam propagation. For a Kerr crystal of length  $L$ , the nonlinear phase shift is given by

$$\Delta\phi_{\text{kerr}} = (1/2)k_1 L n_2 \rho_{\text{1pk}}^2. \quad (12)$$

The comparison between (11) and (12) shows that the ratio between the second order and the Kerr shift increases linearly with the crystal length; thus the comparison between these effects can only be made for individual samples.

For a typical laser host crystal such as the Ti:sapphire ( $n_2 = 3 \times 10^{-20} \text{ m}^2 \text{ W}^{-1} = 1.26 \times 10^{-20} \text{ esu}$  [13]), a 1 mm long sample in the same experimental situation would originate a phase shift of only  $8 \times 10^{-3}$ , i.e. about 20 times lower than the observed second-order phase shift. The ratio is even more favorable when considering others laser crystal such as the Cr:LiSAF ( $n_2 \approx 0.5 \times 10^{-20} \text{ m}^2 \text{ W}^{-1}$ ) and Cr:LiCAF ( $n_2 \approx 0.6 \times 10^{-20} \text{ m}^2 \text{ W}^{-1}$ ) [14], whose Kerr-lens self mode locking operation is quite difficult to achieve [15].

On the other hand, the usual arrangement with an intensity-dependent lens and spatial filter, commonly employed to achieve the fast saturable absorber action can ensure a pulse shortening effect as long as the nonlinearity response can be considered as instantaneous with respect to the fundamental pulse. For the electronic Kerr effect this requirement is fulfilled even in a 10 fs time scale, whereas for the second order effect this assumption is no longer valid when the fundamental pulse duration approaches the limit set by the propagation delay between the  $\omega$  and the  $2\omega$  pulses introduced by the GVM. For the LBO cut for type I phase matching at 790 nm this limit is about 120 fs/mm. Therefore, the length of the crystal to be employed as a passive modulator has to be matched to the desired pulse length.

## 5. Conclusions

The experimental result exposed above shows that during the second pass into the nonlinear crystal, the interaction of the fundamental field with the second harmonic signal, in phase-matching conditions, determines an effective transverse modulation in phase and amplitude of the beam profile, affecting its subsequent propagation. The magnitude and sign of the modulations can be controlled as a function of the field phase difference  $\Theta$ . The effect of the nonlinear modulation on the beam propagation in the limit of low conversion efficiency can be described by means of the Gaussian

decomposition method already introduced in the frame of the z-scan experimental technique.

Then the main advantage offered by this technique is that the achievable values of the lens effect are much higher than those achievable with the usual Kerr media. The comparison becomes even more favorable for increasing crystal lengths. Furthermore, the superimposed phase profile can be tapered independently from the fundamental field intensity, as it depends from the amplitude profile of the second harmonic field, allowing for a more flexible design.

This technique appears particularly promising to achieve the passive mode locking in the 0.1–10 ps time scale, where for a given pulse energy the quadratic dependence with respect to the crystal length allows to compensate for the reduced peak power level.

## References

- [1] H.J. Bakker, P.C.M. Planken, L. Kuipers and A. Lagendijk, *Phys. Rev. A* 42 (1990) 7.
- [2] R. DeSalvo, D.J. Hagan, M. Sheik-Bahae, G. Stegeman and E.W. Van Stryland, *Optics Lett.* 17 (1992) 28.
- [3] D. Pierrottet, B. Berman, M. Vannini and D. McGraw, *Optics Lett.* 18 (1993) 263.
- [4] D.J. Hagan, Z. Wang, G. Stegeman and E.W. Van Stryland, *Optics Lett.* 19 (1994) 17.
- [5] K.A. Stankov and J. Jethwa, *Optics Comm.* 66 (1988) 1.
- [6] K.A. Stankov, V.P. Tzolov and M.G. Mirkov, *Optics Lett.* 16 (1991) 14.
- [7] G. Toci, D. McGraw, R. Pini, R. Salimbeni and M. Vannini, *Optics Lett.* to be published.
- [8] J.A. Armstrong, N. Bloembergen, J. Ducuing and P.S. Pershan, *Phys. Rev.* 127 (1962) 1918.
- [9] M. Sheik-Bahae, A.A. Said, T.H. Wei, D.J. Hagan and E.W. Van Stryland, *IEEE J. Quantum Electron.* 26 (1990) 4.
- [10] S.P. Velsko, M. Webb, L. Davis and C. Huang, *IEEE J. Quantum Electron.* 27 (1991) 9.
- [11] D.W. Chen and J.T. Lin, *IEEE J. Quantum Electron.* 29 (1993) 2.
- [12] A. Agnesi, G.C. Reali and A. Tomaselli, *Optics Lett.* 17 (1992) 24.
- [13] K.H. Lin and W.F. Hsieh, *J. Opt. Soc. Am. B* 11 (1994) 5.
- [14] M. Richardson, M.J. Soileau, R. De Salvo, S. Garnov, D.J. Hagan, S. Klimentov, K. Richardson, M. Sheik-Bahae, A.A. Said, E.W. Van Stryland and B.H.T. Chai, *Proc. SPIE* 1848 (1992) 392.
- [15] N.H. Rizvi, P.M.W. French, J.R. Taylor, P.J. Delfyett and L.T. Florez, *Optics Lett.* 18 (1993) 12.